Received: 24 June 2021 | Revised: 21 September 2021 | Accepted: 13 October 2021

DOI: 10.1111/ina.12950

ORIGINAL ARTICLE

WILEY

# Quantifying the effectiveness of desk dividers in reducing droplet and airborne virus transmission

Wenxin Li[1] | Adrian Chong[1] | Bertrand Lasternas[1] | Thian Guan Peck[2] | Kwok Wai Tham[1]

[1]Department of the Built Environment, School of Design and Environment, National University of Singapore, Singapore, 117566, Singapore

[2]Office of Safety, Health and Environment, National University of Singapore, Singapore, 119246, Singapore

**Correspondence**
Adrian Chong, Department of the Built Environment, School of Design and Environment, National University of Singapore, 4 Architecture Drive, Singapore City 117566, Singapore.
Email: adrian.chong@nus.edu.sg

**Funding information**
National University of Singapore

## Abstract

The utilization of physical dividers has been recommended as a practical approach to reducing the droplet and aerosol transmissions of the COVID-19 virus (SARS-CoV-2). This study conducted a series of experiments using video recording with a high-speed camera, particle image velocimetry (PIV) technique, and concentration measurements. The effectiveness of Perspex desk dividers impeding the transient transmission during coughing in five representative layouts was investigated. The results showed that the divider effectively protected the exposed person from an infector's cough seated in a face-to-face arrangement at a distance of 1.5 m. The aerosol concentration at the breathing zone was reduced by 99% compared to the layout without dividers. However, the reflection of aerosols from the dividers increased the exposure risk to the person seated beside the infector. Such risk was substantially reduced if the dividers were placed parallel between the infector and exposed person seated side-by-side. When the exposed person was staggered (face-to-face but displaced sideways laterally) to the infector with a 0.55-m lateral distance, the dividers reduced the potential exposure at the breathing zone by 60%. Considering the effectiveness in exposure reduction, the staggered configuration of desk dividers between the infector and exposed persons offers the best reduction to exposure.

**KEYWORDS**
airborne transmission, cough, dividers, exposure risk, high-speed camera, particle image velocimetry

## 1 | INTRODUCTION

The current COVID-19 pandemic poses severe threats to human well-being and has caused significant economic losses worldwide. The disease is caused by the SARS-CoV-2 virus, mainly transmitted through fomites, large droplets, and aerosols.[1] The infectious respiratory droplets and aerosols are classified by their aerodynamic diameters: the former have diameters of larger than 5 μm and the latter smaller than 5 μm.[2] Particles of various sizes also behave differently in both the indoor environment and breathing zone. Inside an indoor environment, droplets with a 100-μm diameter took 10 s to fall 3 m to the floor, and those with a 10-μm diameter took 17 m. In contrast, particles with a diameter of between 1 and 3 μm remained suspended almost indefinitely in the turbulent cloud.[3]

Violent exhalations (coughs and sneezes) release multiphase turbulent buoyant clouds with suspended droplets of various sizes.[4] The cloud evolution is first dominated by brief jet-like dynamics and followed by longer-lasting puff dynamics. The first ejection phase corresponds to the high-speed release of the payload, and the second evolution phase is characterized by the

self-similar growth of the puff cloud. Droplets of all sizes settle continuously to contaminate surfaces throughout the cloud's evolution, while smaller droplets evaporate into droplet nuclei and are suspended within the turbulent gas cloud, extending their range to reach the heights of the ventilation systems.[5] To minimize the droplet and aerosol transmissions, ventilation, personal protective equipment, and physical distancing have been highlighted during the ongoing pandemic. The physical distance between people is suggested as at least 1 m by the World Health Organization (WHO)[6] and 1.8 m by the US Centers for Disease Control and Prevention (CDC).[7] However, the recommended distance may be underestimated due to the ignorance of the possible aerosols conveyed by a high-momentum cloud.[5] For scenarios where it is not feasible to keep a physical distance or wear a mask, WHO recommends installing separate and transparent physical dividers.[8] The dividers in the middle of a table or between customers can reduce the possible infection caused by the droplet cloud coughed out by the person across the table.[9]

Dividers have been experimentally and numerically evaluated to reduce airborne transmission. Li et al.[10] simulated the transport of several consecutive coughs from the infector toward an exposed person seated face-to-face 1.5 m away. The desk divider effectively protected and reduced the inhaled dose of the exposed person. A recent study[11] simulated the steady-state aerosol transmission in canteens with cross-divider installed dining tables. The dividers showed limited effects on blocking the path of long-distance aerosol transmission, which gathered the aerosols in the breathing zone inside the partitioned space and left the next diner with certain infection risk. The hospital curtain designed for privacy protection and widely used to separate the patients in hospital wards can be construed as a form of divider of aerosol cross-transmission. A bioaerosol deposition test conducted by King et al.[12] showed that a plastic curtain installed in a two-bed hospital room could effectively reduce cross-contamination between neighboring patient zones. Computational fluid dynamics (CFD) simulations[13] predicted that the curtain between two beds could reduce the peak concentration for each neighboring patient by up to 65% during a bioaerosol dispersion process.

However, though physical dividers were found to alleviate the cross-infection in the overall space, they might create stagnant or recirculating flow, resulting in virus accumulation close to the source. For example, Gilkeson et al.[14] conducted pulse-injection tracer gas experiments in naturally ventilated hospital wards, and the results showed that while the tracer gas concentrations reduced behind the divider, they increased in both the vicinity and downstream of the source. Similarly, installing full-height dividers between two beds to reduce the particle transmission between areas of the room was simulated and showed increasing risk at proximity to the patient. Another CFD study[15] showed that dividers between the beds generally reduced the average concentration while increasing the concentration at the beds opposite and adjacent to the source; such effects would be enhanced by increasing the ventilation rate. In a special case with a ceiling-mounted semi-circular inlet diffuser, the dividers even increased the risk to the healthcare personnel if placed parallel to the recirculating flow.[16] Most of the existing studies of physical dividers are on hospital curtains,[13,14,16,17] and some adopted full-height curtains,[13,17] to separate the patients lying on the bed, while very limited studies focused on the performance of desk dividers.[10,11] The majority of these studies focused on aerosol transmission only[11–13,17] or analyzed with CFD simulations.[10,11,13,15,17] Since the dividers show the potential to reduce the infection risks, and their impacts are sensitive to the relative locations to the source,[14,15] the objectives of this experimental study are to:

- Investigate the characteristics of the droplet and aerosol transmissions in five representative desk divider layouts.
- Compare the exposure concentrations of the exposed person in scenarios with different divider layouts.
- Provide suggestions on using desk dividers.

**Practical Implications**

- The effectiveness of dividers on impeding droplet and aerosol transmissions has been qualified and quantified in this study, which can guide its practical application.
- The transient characteristics of the droplet and aerosol transmissions between room occupants with or without dividers can improve our understanding of airborne transmission.
- The obtained knowledge can contribute to improving the control measures during the current pandemic.

## 2 | METHODS

### 2.1 | Representative divider layouts

This study experimentally investigates the characteristics of aerosol and droplet transmissions and the divider effectiveness in five representative layouts with commercially available Perspex dividers (0.6 m × 0.6 m). These layouts consider various relative locations of the infector and the exposed person with different physical distancing, which are:

- Face-to-face layout (Figure 1A): The exposed person is seated opposite the infector at a physical distance of 1.5 m, a threshold distance often used to distinguish between short- and long-range airborne routes.[18] The distance between the infector and the divider was 0.6 m.
- Staggered layout (Figure 1B): The exposed person is seated opposite but staggered to the infector with a lateral distance (in

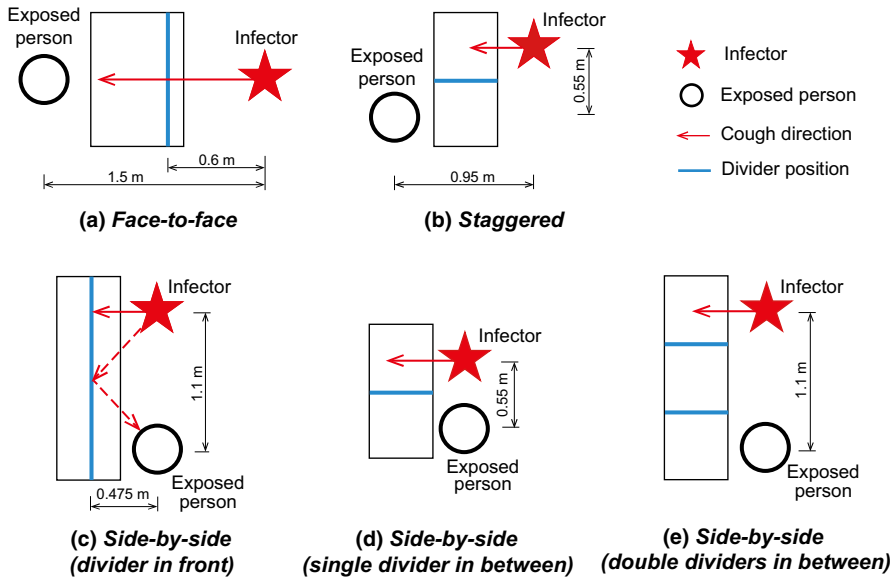


**FIGURE 1** Five representative layouts of Perspex dividers: (A) face-to-face, (B) staggered, (C) side-by-side (divider in front), (D) side-by-side (single divider in between), and (E) side-by-side (double dividers in between)

**TABLE 1** Experimental equipment used in this study

| Devices | Experiments | | | Purpose |
|---|---|---|---|---|
| | High-speed camera recording | PIV | Aerosol measurements | |
| Breathing thermal manikin | ✓ | ✓ | ✓ | Simulating the exposed person |
| Cough machine | ✓ | ✓ | ✓ | Simulating the infector |
| High-speed camera | ✓ | | | Recording |
| PIV technique | | ✓ | | Visualizing particle distribution, quantifying velocity vector |
| Aerosol spectrometer | | | ✓ | Measuring particle concentration at the breathing zone of the exposed person |

Abbreviation: PIV, particle image velocimetry.

the face-to-face direction) of 0.55 m and a longitudinal distance of 0.95 m. The distances were selected based on the typical table size (length 0.75 m × width 0.55 m × height 0.74 m) used in a canteen in the National University of Singapore (NUS). A distance of 0.1 m was considered from the person's abdomen to the table.

- Side-by-side layout where the exposed person and the infector are seated side-by-side in three distinct layouts that include:
  a. Divider in front (Figure 1C): A divider was placed in front while maintaining a physical distance of 1.1 m between the infector and exposed person. The distance between the divider and the infector/exposed person was 0.475 m.
  b. Single divider in between (Figure 1D): A single divider was placed between the infector and the exposed person. The lateral distance between the infector and the exposed person was 0.55 m.
  c. Double dividers in between (Figure 1E): Two dividers were placed between the infector and the exposed person. The lateral distance between the infector and the exposed person was 1.1 m.

For the face-to-face, staggered, and side-by-side (double dividers in between) divider layouts, additional tests without dividers were conducted for comparison.

## 2.2 | Experimental site

The experiments were conducted in a 9.9 m × 6.3 m × 3.7 m classroom in the School of Design and Environment 4 (SDE4) building at the NUS. During the experiments, air temperature and relative humidity were 27 ± 0.5°C and between 70% and 85%, respectively. The building adopts a dedicated outdoor air system (DOAS) with 100% outdoor air supplied. Air is exhausted via pressure-activated openings, and there is no recirculation. The air change per hour (ACH) of the room was measured to be 4.18 (~950 CMH).[19] To minimize the influence of internally generated air currents, all the experiments were conducted at almost the same location away from the supply diffusers. Before all the experiments, velocities at the representative points of the occupied area were measured through two sampling points at 1.1-m and one at 1.7-m height. These three sampling points all gave

similar velocities of 0.4 m/s. With an additional point at 1.7-m height, all the four sampling points gave similar temperatures, which were averaged to be 26.6°C.

## 2.3 | Experimental equipment

In this study, a breathing thermal manikin was used to simulate the exposed person, hereinafter referred to as the exposed person. As shown in Table 1, the droplets and aerosols produced by a cough machine were used to simulate the cough from an infected person, hereinafter referred to as the infector. The transient cough process was recorded using a high-speed camera and PIV. Aerosol concentration at the breathing zone was also measured using aerosol spectrometers.

The female-shaped breathing thermal manikin (P.T. Teknik Limited, Denmark) was dressed in 0.5 clo (short-haired wig, short sleeve shirt, pants, underwear, socks, and shoes) to emulate a typical office worker in Singapore.[20] The manikin has 26 body segments that can be heated and controlled individually. The mode of operation was set to "comfort control," which kept the surface temperatures close to a person's skin temperature in a state of thermal comfort.[21] The average body surface temperature was measured to be 34.4°C, and the ambient temperature was kept at 26.6°C during all the experiments. The generated heat power created a bodily thermal plume that simulated realistic free convection flow around the human body. With a set of artificial lungs, the manikin simulated inhalation through the nose and exhalation through the mouth. A typical value of breathing rate for a person of 6.0 L/min was used. Each respiratory cycle consisted of 2.5-s inhalation, 2.5-s exhalation, and a 1-s break. The manikin was set to breathe continuously throughout the experiments. The same tilted position of the thermal manikin was kept in all experiments to keep the manikin's nose at 1.1-m height.

Coughing was simulated with a cough machine that replicated the initial droplet size reported by Chao et al.[22] (Figure 2) and the initial cough velocity reported by Zhu et al.,[23] where more than 6.7 mg of saliva was expelled at speeds of up to 22 m/s with an average of 11.2 m/s. The cough machine was developed by the Hong Kong University of Science and Technology, Research and Design Corporation Limited, and had been used in previous studies.[24–26] Separately, experiments conducted by Holmgren et al.[27] showed that expiratory droplets evaporated to about 50% of their original diameter (to approximately 10% of their original volume). Hence, the expiratory fluid was simulated with a mixture of water (90% of the total volume) and glycerin (10% of the total volume) to closely resemble human saliva properties and its evaporation. The mixture of two fluids was discharged through an air-atomizing nozzle that generated puffs of droplets with varying size and velocity distributions. The release of gas and liquid phase simulating a cough lasted for 0.55 s. The cough jet was expelled horizontally from the nozzle of the cough machine. The cough machine did not have any heating element; thus, the generated multiphase flow had a temperature as the room ambient temperature of 27 ± 0.5°C. Repeatability tests were performed to ensure that the number and size distribution of the cough droplets do not vary substantially across two consecutive releases.

The high-speed camera (Photron SA1.1 camera, Dynamic Analysis System, Pte Ltd) with an 85-mm AF Nikkor lens (Nikon Inc.) was used to capture the full image of the transmission process.

The PIV technique was used to investigate the instantaneous velocity field. The PIV system consisted of the following components:

- Dual yttrium-aluminum-garnet (YAG) laser (New Wave Research, Inc.) with a 190-mJ double pulse and a 15-Hz frequency
- Light-sheet optics with a 532-nm wavelength
- Synchronizer
- Charge-coupled device (CCD) camera (2MP TSI Power View Plus, TSI Inc.) with a 50-mm AF Nikkor lens (Nikon Inc.)

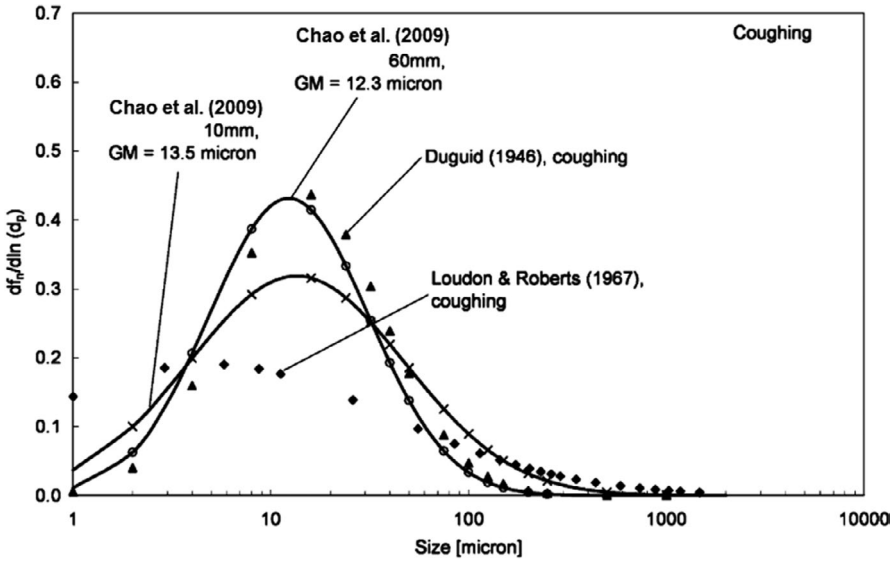


FIGURE 2 Droplet size distribution of the cough generated by the cough machine used in this study, adopted from Chao et al.[22] (reproduced from "Characterization of expiration air jets and droplet size distributions immediately at the mouth opening" by Chao et al. 2009, *Journal of aerosol science*, 40.2, p. 122–133. Copyright 2008 by Elsevier with permission)

- Computer

The PIV laser was aligned with the thermal manikin's vertical axis to illuminate invading cough droplets in the 2D plane. As cough droplets reflect light into the orthogonally positioned CCD camera, their corresponding velocity vectors represent indoor airflow interactions. The targeted measurement area was around 0.5 m × 0.35 m. These images captured by the CCD camera were post-processed using INSIGHT 4G software from TSI Inc.

An aerosol spectrometer (Model Grimm 1.108 and 1.109; Aerosol Technik GmbH, Ainring, Germany) was used to measure the real-time aerosol concentration in the breathing zone of the exposed person (thermal manikin). The aerosol spectrometer has 31 size channels, a sampling rate of 1.2 L/min, and a reproducibility rate of 2%. Measurements of particles with diameters between 0.25 and 2.5 μm were obtained by activating 16 of the 31 lower-sized channels (Model Grimm 1.109) at a measurement frequency of 1 s. Measurements of particles with diameters between 0.265 and 34.0 μm were obtained using another spectrometer (Model Grimm 1.108) by activating all 31 size channels but at a measurement frequency of 6 s.

## 2.4 | Experimental design

Figure 3 shows the experimental setup of all these experiments conducted in the face-to-face layout. The breathing thermal manikin was seated on a chair with a desk in front. Directly opposite the manikin was the cough machine, whose nozzle was fixed at 1.1 m (nose-to-ground height of a seated manikin) above the ground. For a better quality of the experimental data, separate experiments were conducted for the high-speed camera recordings, PIV measurements, and particle measurements (Table 2). In each test, the cough started after indoor airflow distribution had reached steady-state conditions, as had been shown by Pantelic et al.[24] Specifically:

1. High-speed camera recordings. A high-speed camera was used for a broader view to cover the 1.5-m particle transmission from the infector (cough machine) to the exposed person (thermal breathing manikin). Recordings have been conducted for all five representative layouts.
2. PIV measurements. A camera, computer, synchronizer, and laser were used to capture the detailed particle movements at the breathing zone (500 mm × 350 mm). The PIV measurements were conducted for all five layouts, and the generated pseudo-color images and vector fields[25] were used to analyze the transmission characteristics close to the exposed person.
3. Aerosols at manikin's breathing zone were measured with an aerosol sampling probe positioned 5 mm below the tip of the manikin's nose.

Prior to the cough injection, additional 20-s particle measurements were averaged and used as the background particle level. Particles of size ranging between 0.25 and 2.5 μm were measured by spectrometer Model Grimm 1.109 for 30 s for all five layouts. For a broader particle diameter between 0.265 and 34 μm, additional measurements were conducted by spectrometer Model Grimm 1.108 for the face-to-face and side-by-side (double dividers) layouts with/without dividers. These measurements were conducted every 6 s over a 60-s duration. These 30/60-s measurements were found to be sufficient for the concentration level to drop back to the background level during coughing. The measurement error of the aerosol measurement system was calculated to be around 11%.[28] The possible experimental uncertainties included the constant error from the testing equipment and the random error from the nozzle angle and flow volume of the cough machine.

For each layout, the tests were repeated for robustness. Specifically, the PIV measurements were repeated three times. The 1-s particle measurements were repeated ten times for the face-to-face layouts and side-by-side layouts with a divider in front and double divider in between; five times for the staggered layouts and side-by-side layout with a single divider in between. The 6-s particle measurements were repeated ten times for the face-to-face layout without dividers, five times for the layout with dividers, and three times for the side-by-side layouts with/without dividers.

## 2.5 | Data processing

All the aerosol measurements consisted of a 20-s background measurement followed by a 30-s cough exposure process (for particle size 0.25–2.5 μm) at a sampling rate of one measurement each second (by Grimm 1.109). Additionally, for the face-to-face and side-by-side (double dividers) layouts with/without dividers measurement (particle diameter between 0.265 and 34 μm) was undertaken at a sampling frequency of one measurement every 6 s (by Grimm 1.108). The cough exposure processes were identified as a 30/60-s duration after the *starting moment* (at background level), and the moment when particle count reached peak value was identified as the *peak exposure moment*. To minimize the uncertainties and focus on the particle count variations during the exposure, the particle count at the *starting moment* was deducted from the values at every second of the exposure duration. Data from the 20-s background concentration measurements were used in conjunction with the data associated with the initial rise in concentration levels to determine the *starting moment*, which could be decided by two methods based on the difference between the particle counts at the *starting* and *peak exposure* moments for each scenario:

1. The *starting moments* were detected automatically through the R programming language (RStudio, version 4.0.2) for tests with significantly increased particle counts after the exposure. This method could directly and accurately capture the particle count variations close to the exposed person (manikin), and was applied to the 1-s interval tests for the face-to-face layout without divider and side-by-side layout with divider in front. Specifically, the particle counts of these tests increased drastically after the exposure, and

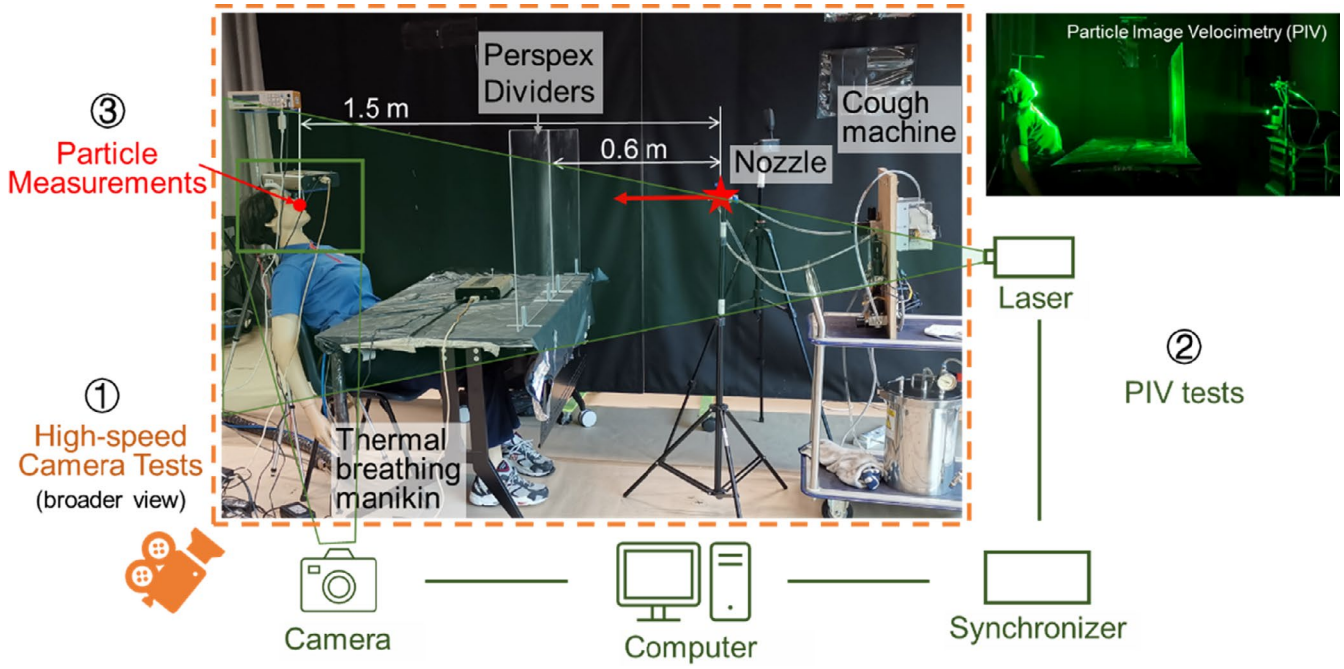


FIGURE 3 Schematic of the experimental setup in the face-to-face layout: (1) High-speed camera recordings (device: high-speed camera) for a broad view to cover the 1.5-m particle transmission from the infector (cough machine) to the exposed person (thermal breathing manikin); (2) particle image velocimetry (PIV) measurements (devices: camera, computer, synchronizer, and laser) to capture the particle transmission at the breathing zone (500 mm × 350 mm) (photograph in the top-right corner shows the experiment with the laser turned on); (3) particles at manikin's breathing zone were measured with an aerosol sampling probe positioned 5 mm below the tip of manikin's nose

TABLE 2 Experiments conducted in this study

| Layouts | | High-speed camera recordings | PIV measurements | Aerosol measurements | | Comparison with no divider scenario (recordings and aerosol measurements only) |
|---|---|---|---|---|---|---|
| | | | | Grimm 1.108 | Grimm 1.109 | |
| Face-to-face | | ✓ | ✓ | ✓ | ✓ | ✓ (Grimm 1.108, 1.109) |
| Staggered | | ✓ | ✓ | | ✓ | ✓ (Grimm 1.109) |
| Side-by-side | Divider in front | | ✓ | | ✓ | |
| | Single divider in between | | ✓ | | ✓ | |
| | Double dividers in between | ✓ | ✓ | ✓ | ✓ | ✓ (Grimm 1.108) |

Abbreviation: PIV, particle image velocimetry.

then the peak value (for all diameters) denoted the *peak exposure moment*. By averaging the first 20-s background particle counts, the mean $\mu$ and standard deviation $\sigma$ were calculated to represent the background level. The *starting moment* of the coughing process was denoted as the closest moment when the background-level particle counts rose above the three-standard deviation value below the *peak exposure moment* ($\mu \pm 3\sigma$, 99.7% probability). Thus, all the particle counts of different diameters were deducted by their corresponding numbers at the *starting moment*. The 30-s data sequence from the *starting moment* was selected to show the particle number variation of a single cough process.

2. The *starting moments* used the recorded moments of starting the cough machine. By neglecting the transmission time from the infector (cough machine) to the exposed person (manikin), this method provided an alternative for scenarios that were not easy for automatic detection due to the slight particle count variations. These include the 1-s tests of "face-to-face with divider," "side-by-side with one/double divider in-between," and "staggered with/without divider" layouts, and all the 6-s measurements. It was reasonable for the 6-s measurements, since the 6-s interval allowed the cough droplets to transmit from the infector (cough machine) to the exposed person (manikin). Similarly, the particle counts during the 30/60-s exposure process were deducted by that of the *starting moment* for each cough process.

Since the aerosol measurements of the 30/60-s cough exposure process were repeated for each experimental scenario, the particle

counts for the sets of measurement (either 1 or 6 s) were averaged, respectively. The abnormal repeated tests caused by the sudden gas/power off of the cough machine were excluded. All the data and codes are available at https://github.com/ideas-lab-nus/partition-virus.

The unequal variance two-tailed *t*-tests were used to determine if there was a statistically significant difference between the means of two aerosol measurement groups. The *t*-test took a sample from each of the two sets with a null hypothesis that the two means were equal. The assumed null hypothesis was accepted or rejected accordingly by comparing the calculated values against the standard values. The following measurements were compared:

- Staggered layout with divider vs. Staggered layout without divider
- Face-to-face layout without divider versus Side-by-side layout with the divider in front
- Side-by-side layout with divider vs. Side-by-side layout without divider
- Side-by-side layout with one divider (with a 0.55-m distance between the infector and the exposed person) versus Side-by-side layout with two dividers (with a 1.1-m distance between the infector and the exposed person)

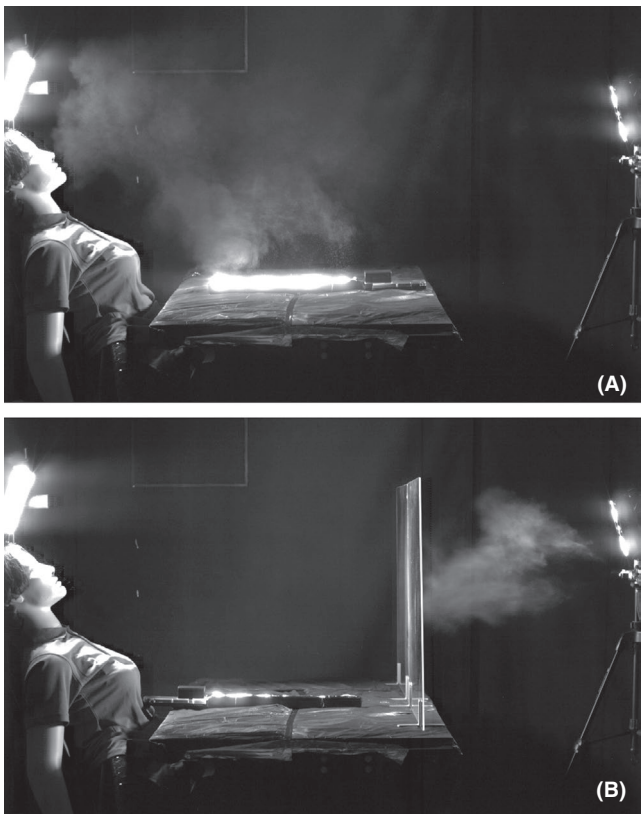


**FIGURE 4** Images recorded by the high-speed camera (A) without and (B) with a divider in the face-to-face layout at the riskiest exposure moment

## 3 | RESULTS

### 3.1 | Face-to-face

Figure 4 captures still images of the droplet and aerosol transmissions with and without a divider in the face-to-face layout through the high-speed camera. In the scenario without a divider (Figure 4A), the cough machine emitted a cone-like-shaped cloud. The strong momentum-driven jet carried particles to reach and flow slightly higher than the exposed person's head due to the buoyancy of the humid droplets (same temperature as the ambient air). Meanwhile, some droplets were deposited on the table halfway toward the exposed person due to the gravity, and the deposition lasted throughout the exposure period. Small droplets remained suspended in the cloud and circulated therein until they settled out (see Video S1). A closer inspection of the PIV measurements (Figure 5) reveals that a large cluster of particles penetrated the exposed person's breathing zone. The strong momentum drove the cough jet directly toward and reached the exposed person's face at a speed of around 2 m/s. However, with a divider located 0.6 m from the cough machine, the flow from the nozzle impinged onto the divider and dispersed at the infector's side (Figure 4B). Consequently, few particles arrive at the breathing zone of the exposed person in the PIV results (Figure 5).

With the divider installed, the peak aerosol concentrations measured at the breathing zone of the exposed person were significantly reduced by 99% from $2.5 \times 10^6$ to $8 \times 10^3$ counts/L for particles with diameters of 0.25–2.5 μm (Figure 6). Figure 7 shows the size distribution of the total number of particles ranging from 0.265 to 34 μm over an exposure period of 30 s. In the scenario without divider, the aggregated particle number was $1.14 \times 10^6$ counts/L, 95% of which were particles smaller than 2.5 μm and 86% less than 1 μm. However, the aggregated value for the case with divider was $4.6 \times 10^4$ counts/L, 98% of which has a smaller size than 2.5 μm and 95% less than 1 μm.

### 3.2 | Staggered

In the staggered layout, the divider protected the exposed person with a 45% reduction in peak concentration values from $2.96 \times 10^4$ to $1.62 \times 10^4$ counts/L (Figure 8). However, the concentration decreased gently with some fluctuation cycles in the scenario without divider, and the layout with divider returned to the background value quicker than the scenario without the divider. The *t*-test rejected the null hypothesis, indicating that the difference between the aerosol concentrations measured in the staggered layout with and without the divider was statistically significant (Table 3).

### 3.3 | Side-by-side

#### 3.3.1 | Side-by-side (divider in front)

Figure 9 shows the particle dispersion and velocity distribution close to the exposed person at the moments of pre-exposure ($t = t_0$

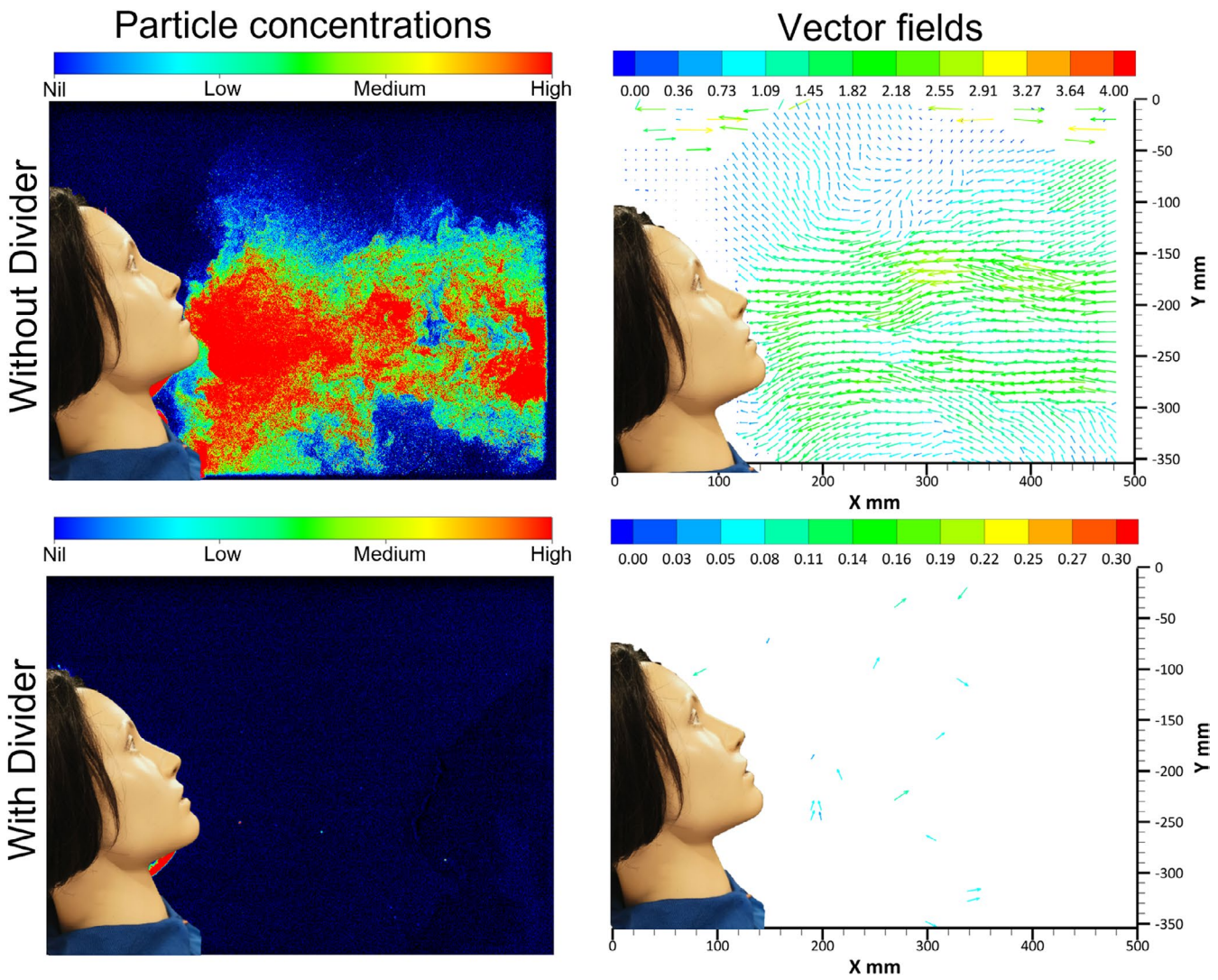


**FIGURE 5** Pseudo-color images and vector fields close to the exposed person (thermal manikin) with and without a divider in the face-to-face layout obtained by the particle image velocimetry (PIV)

- 0.14 s), peak exposure ($t_0$), and end of the exposure ($t = t_0 + 0.91$ s) for the side-by-side (divider in front) layout. With the exposed person seated 1.1 m beside the infector (both facing the divider on the same side), the exposed person was still exposed to the aerosols reflected from the front divider. The particles dispersed toward the front of the exposed person after being reflected from the divider with a velocity of less than 0.2 m/s. This loss in horizontal momentum translates to a longer time during which the particles remain in the vicinity of the exposed person. As indicated in the vector fields, the cough jet traveled directly toward the manikin's head with velocities ranging from 0.05 to 0.2 m/s and dispersed into the background at the end of the exposure ($t = t_0 + 0.91$ s). At the peak exposure moment ($t_0$), the upward airflow affected by the thermal plume could be captured above the manikin's head, where the velocity was ranging from 0.11 to 0.19 m/s.

As shown in Figure 10, particles in the side-by-side (divider in front) layout transmitted toward the exposed person mainly through reflection and dispersion, and had a 51.1% lower peak value than that in the face-to-face layout without divider. Unlike the exponential decay in the face-to-face layout without divider, the particle number in the side-by-side scenario exhibited two phases of decay. The first phase decreased drastically from the 3rd-second peak value (after the cough) to the 9th second. Then the particles lingered and slowly dispersed till the end of the experiment. Meanwhile, the aerosol concentration in the side-by-side layout exceeded that of the face-to-face without divider layout from the 11th second onward, contributing to a higher concentration aggregation for 30 s which was only 22.6% lower than the one in face-to-face without divider layout. It should be noted that the divider placed in the front caused reflection of particles in the side-by-side layout, and significantly increased the particles arriving at the inhalation zone when compared to the scenario without the divider.

As shown in Figure 11, similar number variations were observed by particles in size bins of 0.25–0.5 μm, 0.5–1 μm, and 1–2.5 μm. Specifically, the concentrations of particles with a diameter larger than 0.5 μm in the side-by-side layout also overtook that of the

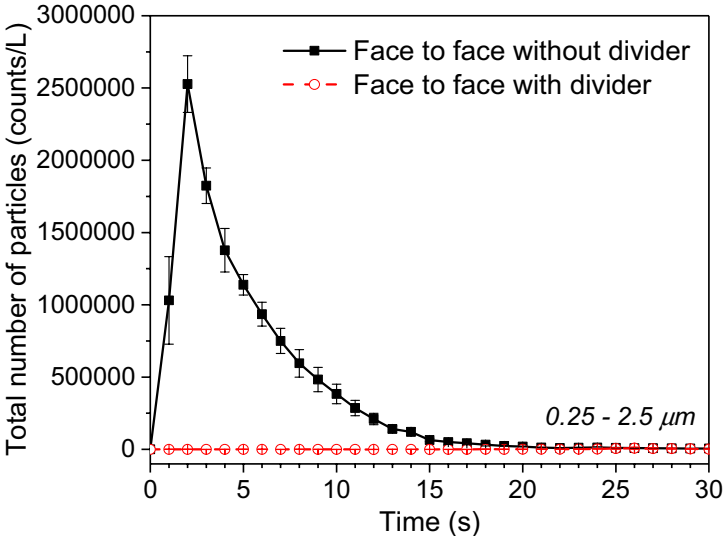


FIGURE 6 Comparisons of total particle number variations between aerosol transmissions with/without divider measured every 1 s ($0.25 \le d \le 2.5$ μm) from aerosol measurements

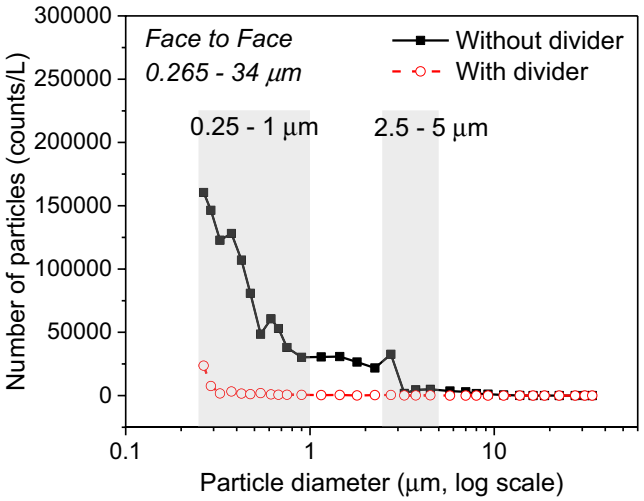


FIGURE 7 Comparisons between aerosol transmissions with/without divider: diameter distributions of the total particles ($0.265 \le d \le 34$ μm) aggregated over the first 30-s exposure period obtained by aerosol measurements with 6-s intervals

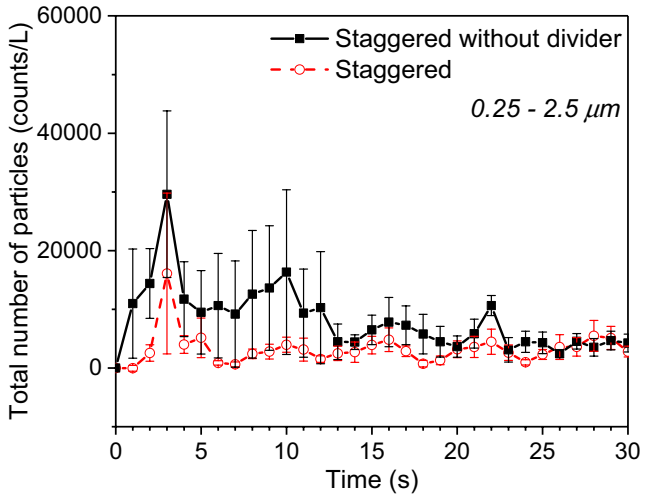


FIGURE 8 The total number of particles between 0.25 and 2.5 μm recorded at the breathing zone of the exposed person (thermal manikin) by every second for 30 s in the staggered layout with/without divider obtained by aerosol measurements

TABLE 3 The *t*-test results of total aerosol numbers between different scenarios

| Comparison between layouts | | *t*-value | *p*-value |
|---|---|---|---|
| Staggered with divider | Staggered without divider | −4.30 | $9.25 \times 10^{-5}$ |
| Face-to-face without divider | Side-by-side with divider in front | 0.69 | 0.49 |
| Side-by-side with divider | Side-by-side without divider | −1.57 | 0.68 |
| Side-by-side with one divider | Side-by-side with two dividers | 3.35 | $1.46 \times 10^{-3}$ |

*The significance level (α) for all *t*-tests is 0.05.

face-to-face without divider layout at 11 s, but their differences were not apparent from the 5th second. Obvious overtaking could be observed in the 0.25–0.5 μm particles, which accounted for 75% of the total measured particles. The overtaking is attributable to the slowed-down rate in the decrease of particle concentrations. Being able to remain suspended in the breathing zone of the exposed person, a large amount of the 0.25–0.5 μm particles took 20 s to decay and return to the background values subsequently.

Additional t-test was conducted for measurements between the side-by-side layout with the divider in front and face-to-face without divider (Table 3). The result failed to reject the null hypothesis and showed no statistically meaningful difference between the two sample means of these layout data at $p = 0.49$.

### 3.3.2 | Side-by-side (divider in between)

Figure 12 shows the effect of the divider on aerosol transmission for the side-by-side (dividers in between) layout. With a physical

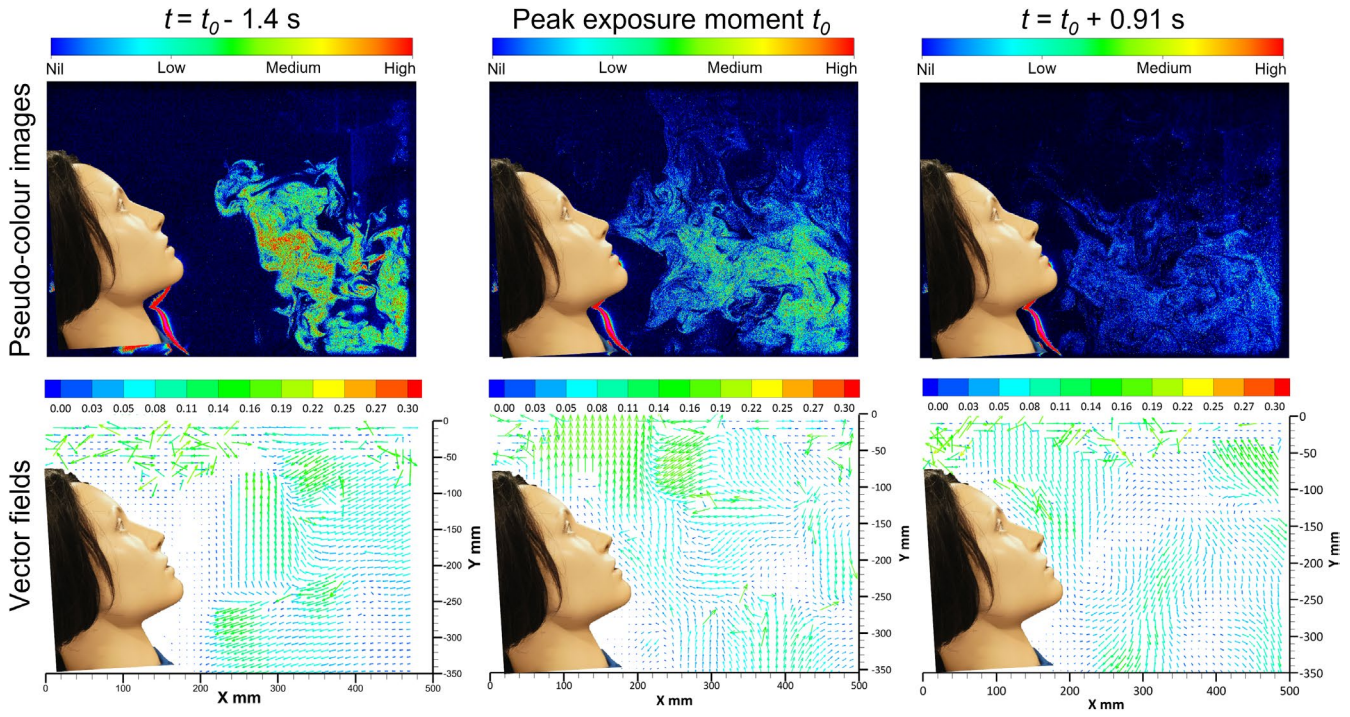


FIGURE 9 Pseudo-color images and vector fields close to the exposed person (manikin) in the side-by-side (divider in front) layout obtained by particle image velocimetry (PIV)

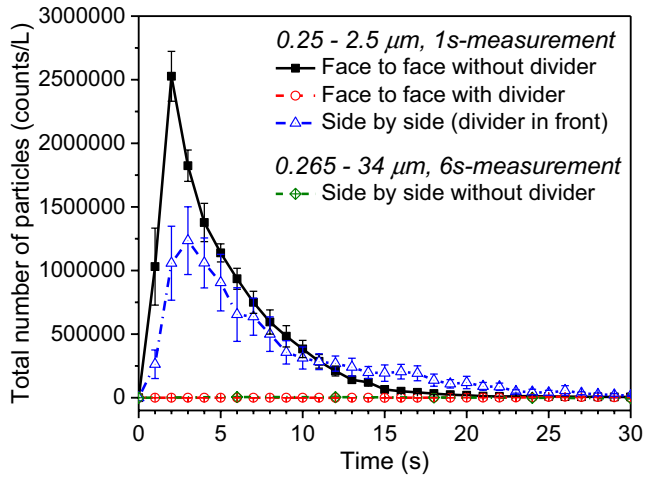


FIGURE 10 Comparison of the total particle (0.25–2.5 μm) concentration at the breathing zone of the exposed person located face-to-face (in red) and side-by-side (in blue) to the infector over 30 s

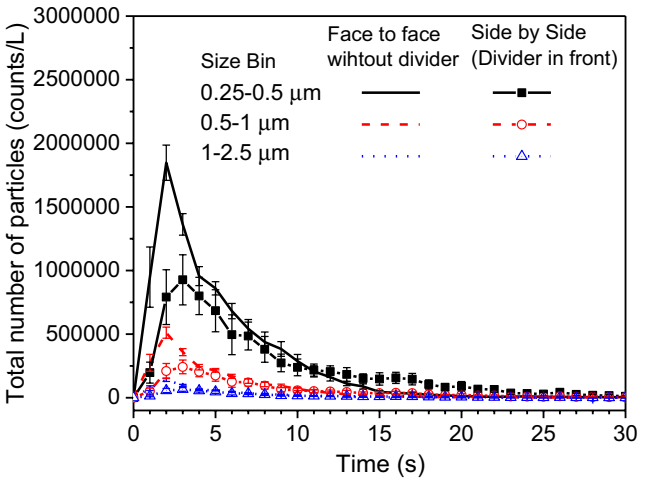


FIGURE 11 Total number comparison of particles in size bins of 0.25–0.5, 0.5–1, and 1–2.5 μm measured at the exposed person's breathing zone in the face-to-face layout without divider and side-by-side layout with the divider in front obtained by aerosol measurements

distance of 1.1 m between the infector (cough machine) and the exposed person (thermal manikin), the visible aerosols could hardly traverse toward the exposed person. Consequently, the divider had an insignificant effect on impeding the lateral particle transmission. This conclusion was further supported by the particle measurements shown in Figure 13A, where scenarios with/without divider gave similar concentrations at the breathing zone. When comparing the particle numbers in different layouts, their background particle numbers were subtracted from the measurements, and the negative values indicated the measurements were lower than the background values. Such fluctuations were reasonable, since the measured particle numbers were strongly affected by the surrounding airflow turbulence. The corresponding hypothesis tests (*t*-test) failed to reject the null hypothesis. The divider application showed no significant difference ($p = 0.68$) in the number of total particles in the breathing zone.

Figure 13B compares the aerosol concentrations at the breathing zone of the exposed person seated 0.55 and 1.1 m to the infector. Since the cough jet had a strong momentum to travel beyond the

region where the exposed person was seated, the breathing zone received few particles in the initial exposures, followed by a quick recovery to the background value. The difference between particle number variations in the side-by-side layout with single/double dividers in between was because of the random fluctuation. The hypothesis tests (*t*-test) were conducted for measurement data of side-by-side layouts with single/double dividers. The tests rejected the null hypothesis, and the 0.55/1.1-m distance with one/two dividers between the infector and exposed person ($p = 1.5 \times 10^{-3}$) showed a statistically significant difference in the number of total particles at the breathing zone.

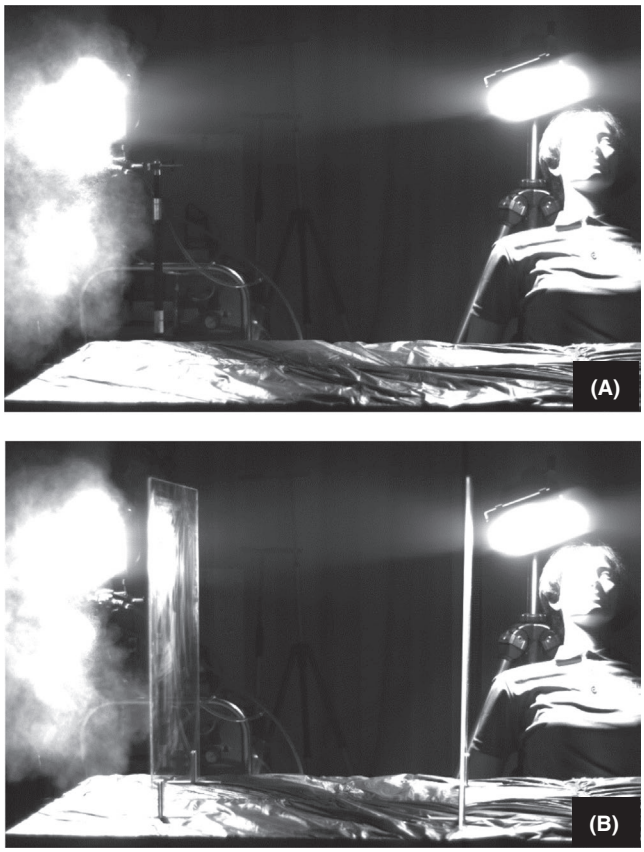


FIGURE 12 High-speed camera recording images of the "side by side" layouts (A) without and (B) with two dividers in between at the riskiest exposure moment

## 3.4 | Aggregated concentration

The SARS-CoV-2 virus has a diameter of 0.1 μm[29] and has been reported to be mainly contained in particles with diameters of 0.25–1.0 μm and >2.5 μm.[30] For comparison, the majority of influenza A viral copies were found in particles smaller than 2.5 μm.[31] Thus, concentrations of the fine particles ranging between 0.25 and 2.5 μm were used to compare the overall particle exposure risks for different divider layouts in this study. For each layout, the particle concentration was calculated as the sum of released cough droplets/aerosol concentration in the breathing zone of the exposed person after a single instance of cough was released:

$$Aggregatedconcentration = \sum_{i=0}^{t_E=30} C_i \quad (1)$$

where $C_{i,s}$ is the particle number measured at the breathing zone at the *ith* second for particles of size $0.25 \le d \le 2.5$ μm and $t_E$ refers to the total exposure time of 30 s in this study.

Figure 14 compares the aggregated concentrations (Equation 1) under different layouts of the dividers. The addition of the divider in the face-to-face and staggered layouts could decrease their aggregated concentrations by 99% and 60%, respectively. However, the side-by-side layout with a divider in front had the maximum

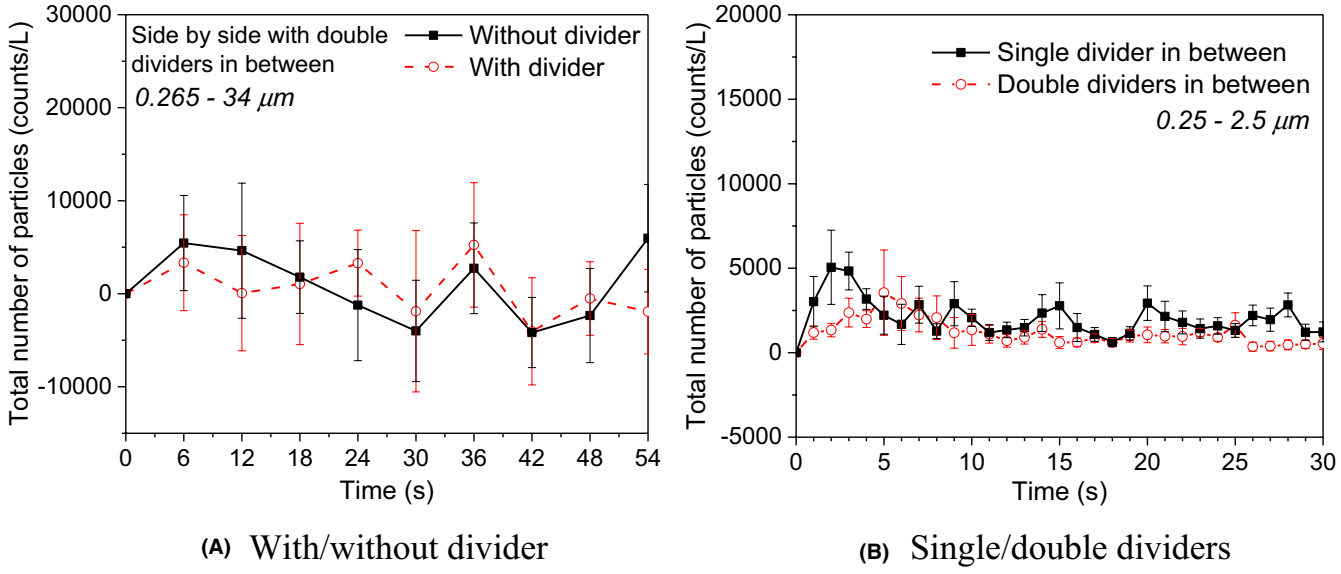


FIGURE 13 Comparisons of particle numbers in the side-by-side layouts (A) with/without divider and (B) with single/double dividers measured at the breathing zone of the exposed person obtained by aerosol measurements

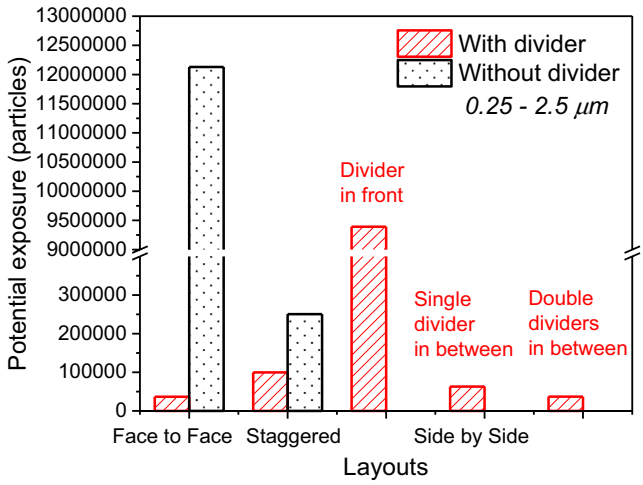


**FIGURE 14** Potential exposure of the particles (0.25–2.5 μm) measured at the breathing zone in layouts of face-to-face, staggered, and side-by-side with/without dividers during the 30-s cough exposure period obtained by aerosol measurements

aggregated concentration among all layouts with the divider, reaching 77% of the directly exposed one without the divider (face-to-face layout without divider). With a distance of over 1 m between the infector and exposed person, the face-to-face layout and double dividers in between the side-by-side layout received lower aggregated concentrations than layouts with closer distances (the staggered and side-by-side layouts with single divider). By avoiding direct exposure by seating on the same side with a divider in between, the side-by-side layout with a single divider in between had a smaller exposure risk compared to the staggered layout. This indicates that the exposure direction and staggering are critical considerations for aggregated concentration exposure.

## 4 | DISCUSSION

### 4.1 | Comparison between different layouts

The unprotected face-to-face scenario has the worst exposure because the momentum-driven aerosol cloud easily traverses the 1.5 m between the infector and the exposed person. Placing a divider inhibits this movement achieving >99% reduction of exposure and offers effective mitigation in close seating arrangements where space constraints prevent larger safe distancing measures from being adopted. The disinfection of the divider is necessary as the impinging "cloud" is likely to cause fomite deposition. However, this configuration poses a significant exposure to an exposed person seated side-by-side on the same side of the divider. The reflected aerosols linger much longer around the exposed person as they have lost most of their horizontal momentum, and therefore take a longer time to traverse the exposed person. Due to the reflection, the dividers installed in the side-by-side layout with a divider in front could accumulate particles locally and contribute to a higher concentration during some time compared to the one without divider. A CFD study[11] gave similar conclusions that the aerosols will gather in the breathing zone inside the partitioned space.

The 60% reduction achieved by the staggered face-to-face scenario with the use of a central divider has the advantage of providing larger desk space and a sense of separation between seated colleagues. However, the residual aerosols beyond the immediate measurement zone of the exposed person continue to pose a challenge as long-range airborne transmission after the "cloud" passes the exposed person.

The double divider scenario for the side-by-side scenario, with a larger lateral distance between the infected and the exposed persons, improves the reduction in aggregated exposure when compared to the single divider with a closer seating arrangement. From the space occupancy consideration, this offers a slight advantage over the single divider scenario.

Considering the costs and potential risks for the surrounding people, it is not appropriate to install the dividers if many people are on the same side of the divider simultaneously. The previous study[10] and recommendations[9] using table dividers are mainly based on the face-to-face layout but focus on the scenario with only one person behind the divider. Thus, the installation of table partitions should consider the surrounding environment (e.g., other occupants, furniture, etc.). Additionally, a more frequent wipe-down is necessary for the face-to-face layout since the partition will have maximum exposure.

In comparison, the staggered layout decreased the aerosol concentration at the breathing zone by 60% without potential reflection risk to the surrounding people. Placing double dividers between the infector and the exposed person had a marginal effect on particles transmitted to the breathing zone of the side-by-side exposed person, and it had a slightly lower aerosol concentration than the side-by-side layout with a single divider considering a larger space occupancy. It can be inferred that the dividers have little effect on impeding the droplets or aerosol transmission in the side-by-side layout beyond a certain distance between the infector and exposed person (e.g., 1.1 m tested in this study). It suggests that the dividers are unnecessary if occupants are appropriately staggered. However, beyond the immediately exposed person, the long-range airborne transmission within the office needs to be considered.

### 4.2 | Diameter distribution of virus particles

In this study, even if the original droplets generated by the infector (cough machine) had a lognormal distribution[22] (Figure 1), most of the particles arriving at the breathing zone of the exposed person had sizes within the sub-micrometer region (0.25–1 μm). It was because compared to the large particles, the small particles could remain suspended in the turbulent cloud,[3] and the time was long enough for them to travel 0.55–1.5 m from the infector to the

exposed person in this study. The sub-micrometer particles were around an order of magnitude more than the larger particles (ranging from 1 μm to 2.5/34 μm). It was supported by a deposition test where small (~2.5 μm) particle bioaerosols were deposited across the room, since they dominated the transmission of infection through indirect contact routes.[12] Since the sub-micrometer particles were more easily inhalable than their larger counterparts, they would contribute to a higher transmission risk. The implications of aerosol particle size distributions can be analyzed for the SARS-CoV-2 virus.

The SARS-CoV-2 aerosols mainly include two size ranges of the particle diameters: 0.25–1.0 μm and >2.5 μm.[30] The relevant aerosol size bins are 0.25 μm ≤ $d$ ≤ 1.0 μm and 2.5 μm ≤ $d$ ≤ 5.0 μm. In the face-to-face layout with/without divider (Figure 7), the divider installation reduced the aggregated particle numbers from 976,144 to 43,654 for 0.25–2.5 μm size bin and from 65,689 to 1,208 for the 2.5–5 μm size bin, respectively. The reductions were more than 95% for both the representative size bins of SARS-CoV-2 aerosols. For both face-to-face layout without divider and side-by-side layout (divider in front), particles ranging from 0.25 to 1 μm accounted for 95% of the total particle number (0.25–2.5 μm). Considering the high concentration and easily inhalable characteristics of the sub-micrometer particles, special attention should be paid to the aerosol transmission during the current COVID-19 pandemic.

### 4.3 | Limitations

The droplets generated by the cough machine have the same temperature as the ambient temperature; thus, the evaporation and particle trajectory attributed to the temperature difference between cough droplets and ambient temperature were ignored in this study. All the experiments in this study were conducted in a small room under almost calm and non-fluctuating conditions. The conclusions were drawn and limited to these application scenarios. The findings may be different since the results are determined by the airflow patterns and boundary effects of the room, which may exhibit different airflow patterns. Meanwhile, this study only investigates the divider's effects on the droplet/aerosol transmissions generated by a single cough; however, their transmission characteristics under gentler expiratory activities such as tidal breathing and talking may differ. The potential exposure at other regions of the room attributable to residual aerosols beyond the exposure of the exposed person is not considered. In reality, cough directions can also vary from the directly forward direction used in this study.

## 5 | CONCLUSION

This study investigated the effects of desk partitions (Perspex divider) on the droplet and aerosol transmissions experimentally during a transient cough process. The transmission characteristics of five representative divider layouts were compared. The high-speed camera tests captured a broad view of the transmission process; the detailed transmission around the exposed person's breathing zone was analyzed with results from PIV measurements; concentrations at the breathing zone were measured to evaluate the potential exposure quantitatively. The conclusions arising from this study are summarized as follows:

1. The face-to-face layout with a divider separation was the most effective layout of using dividers, where the divider reduced 99% of the potential exposure at the breathing zone of the exposed person. However, it was likely to generate a high exposure risk for the exposed person seated beside the infector (i.e., side-by-side layout with a divider in front) due to the reflection, even with a physical distance of more than 1 m.
2. Dividers in the staggered layout can reduce potential exposure at the breathing zone by 60%.
3. The exposure reduction of the side-by-side layout with a single divider in between could be improved by adding one more divider and doubling the lateral distance between the infector and the exposed person. However, beyond a certain lateral distance, the effects of using dividers would be negligible.
4. Sub-micrometer-sized particles (0.25–1 μm) dominated the transmissions arriving at the breathing zone of the exposed person who was more than 1 m away from the infector, and the particle sizes were within the typical infectious size bins of the SARS-CoV-2 virus.

This study conducted all the experiments in a room with a low airflow pattern and with cough considered. Thus, applications in open-air and air-conditioned situations or with gentler expiratory activities (such as tidal breathing and talking) or affected by other human behaviors could perform differently from the conclusions obtained from this study. In addition, the potential exposure at other regions of the room attributable to residual aerosols beyond the exposure of the exposed person is not considered. The evaporation and particle trajectory affected by the temperature difference between cough droplets and ambient temperature were ignored in this study.

### ACKNOWLEDGMENTS

This research is supported by the National University of Singapore, Singapore, under its Office of Safety, Health and Environment (OSHE) (Grant number: R-296-000-223-736). The authors thank Ms. Wei Yi Wu (National University of Singapore) and Dr. Yongchuan Khoo (TSI Instruments Singapore Pte Ltd.) for their technical assistance. The authors also thank Dr. Lei Xu and Ms. Shuxu Qin from the National University of Singapore for their assistance in conducting the experiments.

### CONFLICT OF INTEREST

The authors declare that they have no known competing financial interests or personal relationships that could have appeared to influence the work reported in this paper.

## AUTHOR CONTRIBUTIONS

**Wenxin Li:** Methodology, Formal analysis, Investigation, Writing - original draft, Writing - Review & Editing, Visualization. **Adrian Chong:** Conceptualization, Writing - original draft, Writing - Review & Editing, Supervision, Project administration. **Bertrand Lasternas**: Conceptualization, Resources. **Thian Guan Peck**: Conceptualization. **Kwok Wai Tham**: Writing - original draft, Writing - Review & Editing, Supervision.

## ORCID

*Wenxin Li* https://orcid.org/0000-0001-9866-6713
*Adrian Chong* https://orcid.org/0000-0002-9486-4728
*Kwok Wai Tham* https://orcid.org/0000-0002-2957-1152

## REFERENCES

1. Morawska L, Cao J. Airborne transmission of SARS-CoV-2: the world should face the reality. *Environ Int*. 2020;139:105730.
2. World Health Organization. *Infection prevention and control of epidemic-and pandemic-prone acute respiratory infections in health care*. World Health Organization; 2014.
3. Knight V. Viruses as agents of airborne contagion. *Ann N Y Acad Sci*. 1980;353(1):147-156.
4. Bourouiba L, Dehandschoewercker E, Bush John WM. Violent expiratory events: on coughing and sneezing. *J Fluid Mech*. 2014;745:537-563.
5. Bourouiba L. Turbulent gas clouds and respiratory pathogen emissions: potential implications for reducing transmission of COVID-19. *JAMA*. 2020;323(18):1837-1838.
6. World Health Organization. Coronavirus disease (COVID-19) advice for the public. 2021.
7. Centers for Disease Control and Prevention. Social Distancing. 2020.
8. World Health Organization. *Rational use of personal protective equipment for COVID-19 and considerations during severe shortages: interim guidance, 23 December 2020*. World Health Organization; 2020.
9. Chen Q. Can we migrate COVID-19 spreading risk? *Front Environ Sci Eng*. 2021;15(3):35.
10. Li X, Niu J, Gao N. Characteristics of physical blocking on co-occupant's exposure to respiratory droplet residuals. *J Cent South Univ*. 2012;19(3):645-650.
11. Liu Z, Li R, Wu Y, Ju R, Gao N. Numerical study on the effect of diner divider on the airborne transmission of diseases in canteens. *Energy Build*. 2021;248:111171.
12. King M-F, Noakes C, Sleigh P, Camargo-Valero M. Bioaerosol deposition in single and two-bed hospital rooms: a numerical and experimental study. *Build Environ*. 2013;59:436-447.
13. Ching WH, Leung MKH, Leung DYC, Li Y, Yuen PL. Reducing risk of airborne transmitted infection in hospitals by use of hospital curtains. *Indoor Built Environ*. 2008;17(3):252-259.
14. Gilkeson C, Camargo-Valero M, Pickin L, Noakes C. Measurement of ventilation and airborne infection risk in large naturally ventilated hospital wards. *Build Environ*. 2013;65:35-48.
15. Cheong CH, Lee S. Case study of airborne pathogen dispersion patterns in emergency departments with different ventilation and partition conditions. *Int J Environ Res Public Health*. 2018;15(3):510.
16. Nielsen PV, Li Y, Buus M, Winther FV. Risk of cross-infection in a hospital ward with downward ventilation. *Build Environ*. 2010;45(9):2008-2014.
17. Noakes C, Sleigh P, Escombe A, Beggs C. Use of CFD analysis in modifying a TB ward in Lima, Peru. *Indoor Built Environ*. 2006;15(1):41-47.
18. Liu L, Li Y, Nielsen PV, Wei J, Jensen RL. Short-range airborne transmission of expiratory droplets between two people. *Indoor Air*. 2017;27(2):452-462.
19. Li W, Chong A, Hasama T, et al. Effects of ceiling fans on airborne transmission in an air-conditioned space. *Build Environ*. 2021;198:107887.
20. de Dear RJ, Leow KG, Foo SC. Thermal comfort in the humid tropics: field experiments in air conditioned and naturally ventilated buildings in Singapore. *Int J Biometeorol*. 1991;34(4):259-265.
21. BYTELINE. Manikin manual, version 3.x. https://www.manikin.dk/download/manual.pdf2018. Accessed 20 May 2021.
22. Chao CYH, Wan MP, Morawska L, et al. Characterization of expiration air jets and droplet size distributions immediately at the mouth opening. *J Aerosol Sci*. 2009;40(2):122-133.
23. Zhu S, Kato S, Yang J-H. Study on transport characteristics of saliva droplets produced by coughing in a calm indoor environment. *Build Environ*. 2006;41(12):1691-1702.
24. Pantelic J, Sze-To GN, Tham KW, Chao CY, Khoo YCM. Personalized ventilation as a control measure for airborne transmissible disease spread. *J R Soc Interface*. 2009;6(suppl_6):S715-S726.
25. Pantelic J, Tham KW, Licina D. Effectiveness of a personalized ventilation system in reducing personal exposure against directly released simulated cough droplets. *Indoor Air*. 2015;25(6):683-693.
26. Pantelic J, Tham KW. Adequacy of air change rate as the sole indicator of an air distribution system's effectiveness to mitigate airborne infectious disease transmission caused by a cough release in the room with overhead mixing ventilation: a case study. *HVAC&R Res*. 2013;19(8):947-961.
27. Holmgren H, Bake B, Olin A-C, Ljungström E. Relation between humidity and size of exhaled particles. *J Aerosol Med Pulm Drug Deliv*. 2011;24(5):253-260.
28. Pantelic J. Exposure generated by cough released droplets in the indoor environment-a comparison among four ventilation systems. 2010.
29. Bar-On YM, Flamholz A, Phillips R, Milo R. SARS-CoV-2 (COVID-19) by the numbers. *Elife*. 2020;9:e57309.
30. Liu Y, Ning Z, Chen Y, et al. Aerodynamic analysis of SARS-CoV-2 in two Wuhan hospitals. *Nature*. 2020;582(7813):557-560.
31. Yang W, Elankumaran S, Marr LC. Concentrations and size distributions of airborne influenza A viruses measured indoors at a health centre, a day-care centre and on aeroplanes. *J R Soc Interface*. 2011;8(61):1176-1184.

## SUPPORTING INFORMATION

Additional supporting information may be found in the online version of the article at the publisher's website.

**How to cite this article:** Li W, Chong A, Lasternas B, Peck TG, Tham KW. Quantifying the effectiveness of desk dividers in reducing droplet and airborne virus transmission. *Indoor Air*. 2021;00:1–14. doi:10.1111/ina.12950